

Electromechanical analysis of micromechanical SOI-fabricated RF resonators

T. Lamminmäki^{*}, K. Ruokonen^{*}, I. Tittonen^{*},
T. Mattila^{**}, O. Jaakkola^{**}, A. Oja^{**}, H. Seppä^{**},
P. Seppälä^{***} and J. Kiihamäki^{***}

^{*}Helsinki University of Technology, Metrology Research Institute
P. O. Box 3000, FIN-02015 HUT, Finland, tuomas.lamminmaki@hut.fi

^{**}VTT Automation, P. O. Box 1304, FIN-02044, Finland

^{***}VTT Electronics, P. O. Box 1101, FIN-02044, Finland

ABSTRACT

In this paper, finite element method (FEM) simulations are used to model mechanical properties of MEMS resonators. Using a static displacement analysis the effective spring constant and mass are calculated. Non-linearity of the mechanical restoring force is simulated to analyze large amplitude behavior of the resonator.

Equivalent electrical circuit modeling is used for the simulating the frequency response of the resonators by APLAC RF-circuit simulator [1]. The FEM-calculated effective mass and spring constant are used to calculate equivalent electric circuit values.

FEM and circuit simulation results are compared with the measured response of two example resonator structures; as an example we show detail analysis of clamped-clamped beam resonator operating at 1.6 MHz frequencies with Q-value 30000. Mechanical non-linearities are included in the circuit simulation.

Keywords: electromechanical modeling, FEM, SOI-resonator, equivalent circuit, mechanical non-linearity

1 INTRODUCTION

The rapidly developing telecommunication systems are setting increasing requirements for RF-components in performance, size, cost and integrability. Micromechanical resonators have emerged as a promising technique to meet these demands.

Micromechanical high frequency resonators have usually been fabricated by surface micromechanics, which can be integrated with ICs. In addition, poly-Si provides flexibility in geometry, anchoring and number of structural layers. However, polycrystalline silicon has non-optimal intrinsic quality factor and it is typically processed at high temperatures, which develops stress gradients in film layers due to mismatches in thermal expansion coefficients [2].

To overcome these problems, single-crystal silicon is used in this work. Single-crystal silicon is fully elastic up to fracture resulting in minimal hysteresis in normal temperature area. It has very high intrinsic Q-factor (up to $6 \cdot 10^5$ in room temperature [3]) and the strength of single-

crystal silicon is comparable to that of steel. There have been some efforts [2] to integrate single-crystal silicon micromechanical resonators on standard wafers, but using RFIC (Radio Frequency Integrated Circuit) single-crystal silicon-on-insulator (SOI) wafers integration is easier to implement.

Single-crystal SOI-wafers are very useful material for mechanical RF-resonator applications because SOI has become strategic for low-power, battery-operated portable systems and large-scale integrated logic and memory circuits with sub-half micron features. In addition many integrated micromechanical SOI-CMOS-sensors [4],[5] and integrated dipole antennas [6] have been presented.

The fabrication of micromechanical SOI-resonators operating at high frequencies, fulfilling simultaneously the strict noise performance specifications, remains challenging. Accurate modeling of the resonator structures is required to allow the design of components with the desired properties. Analytic modeling of micromechanical capacitively actuated resonators is complex, since the resonators are described by dynamic, non-linear equations coupling electric and mechanical energy domains.

In this study we have used finite element modeling which provides a very flexible tool for simulation of both mechanical and electrostatical behavior of electromechanical microresonator. With same method very complex geometries can be modeled and optimized. Based on the FEM-calculated mechanical parameters, a equivalent electrical circuit model is used for simulation of resonator dynamic response. Comparison between measured and simulated results shows good agreement indicating reliability of the modeling approach.

2 MODELING

Clamped-clamped beam (bridge) resonator is electrostatically coupled at both sides by the two electrodes A and B (Figure 1). The beam is vibrating in the plane of the silicon wafer (in lateral direction) and first eigenmode is excited and read by the electrodes.

2.1 Analytic modeling

Spring constant of lateral clamped-clamped beam resonator can be calculated by equation

$$k = 16Eh \frac{w^3}{L^3} \quad (1)$$

where E is Young's modulus of silicon ($E_{[100]} = 130$ GPa), h is height ($8 \mu\text{m}$), L length and w width of the beam. First eigenfrequency of clamped-clamped beam is

$$f = 1.03 \sqrt{\frac{E}{\rho}} \frac{w}{L^2} \quad (2)$$

where ρ is the density of the silicon ($\rho_{Si} = 2330 \text{ kg/m}^3$). Eigenfrequency of spring-mass system is

$$f = \frac{1}{2\pi} \sqrt{\frac{k}{m}} \quad (3)$$

where m is effective mass of the mechanical resonator. Value for effective can be derived using equations (1)-(3)

$$m = \frac{k}{(2\pi f)^2} = 0.38\rho(hLw) = 0.38m_0, \quad (4)$$

where m_0 is physical mass of the beam.

2.2 Finite element simulations

Using FEM effective spring constant and eigenfrequencies can easily be simulated for structures of varying size. The linear spring constant k can be calculated by structural analysis simulating the displacement caused by an external force (See Figure 2). The simulations presented have been made using ANSYS FEM-package.

The beam displacement profiles calculated for point-like and distributed loads are shown for an example bridge resonator ($w=3\mu\text{m}$, $L=120\mu\text{m}$) in Figures 3 and 4, respectively. The distributed load represents the capacitive pull by the electrode of length L_e . Difference between these models increases, when ratio L/L_e decreases as shown in Figure 5.

The FEM-calculated mechanical values using the distributed force ($L_e=100 \mu\text{m}$) are shown for two resonator designs ($w=3 \mu\text{m}$, $L=220/120 \mu\text{m}$) in Table 1. The third-order mechanical non-linearity (k_3) was extracted by performing a polynomial fit of the force-displacement function (Figure 2).

1.3 Equivalent electrical circuit simulations

Component values of the equivalent circuit in Figure 6 can be derived by equations

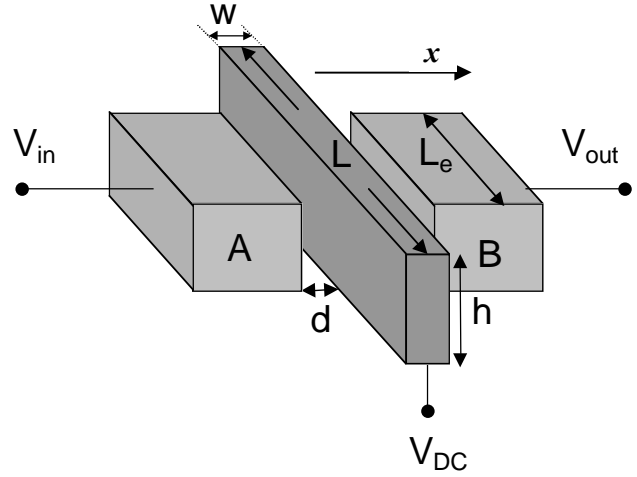


Figure 1: Schematic representation of the bridge resonator.

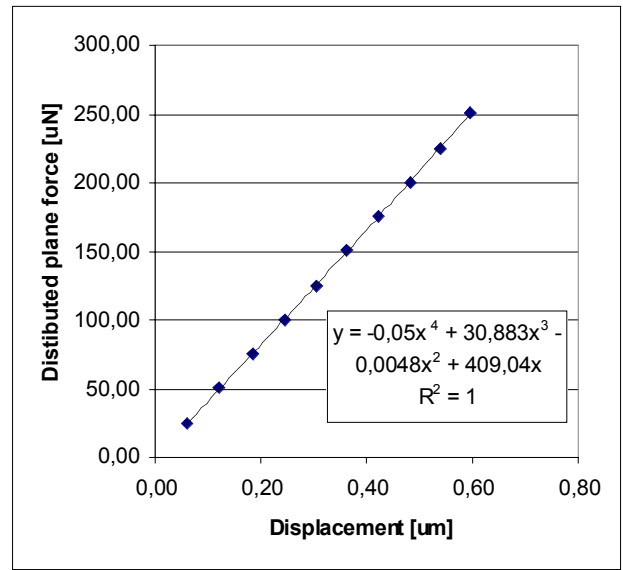


Figure 2: Simulated nonlinear spring constant of the $L=120\mu\text{m}$ resonator.



Figure 3: The deformation profile, when point-like force ($F=300 \mu\text{m}$) is applied at the center of the beam. The shaded areas and associated numbers denote the displacement (in units of μm).



Figure 4: The deformation profile, when distributed force ($F=300 \mu\text{m}$, $L_e=100 \mu\text{m}$) is applied at the center of the beam. The shaded areas and associated numbers denote the displacement (in units of μm).

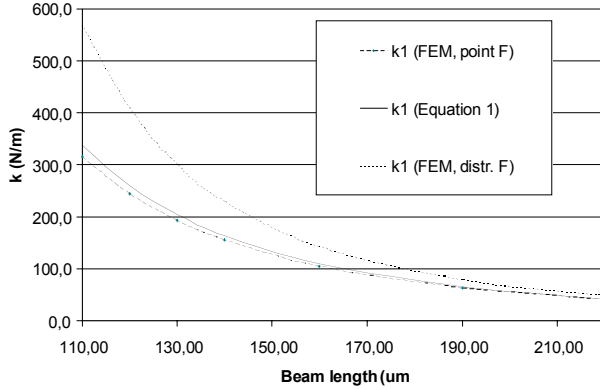


Figure 5: Spring constant k of a bridge resonator as the length L of the bridge is varied. Length of the electrode in the case of distributed force is kept at $L_e=100 \mu\text{m}$.

		Dimension	Type I	Type II
Length	L	$[\mu\text{m}]$	220	120
Width	w	$[\mu\text{m}]$	3	3
Height	h	$[\mu\text{m}]$	8	8
Electrode length	L_e	$[\mu\text{m}]$	100	100
Electrode gap	d	$[\mu\text{m}]$	1	1
Spring constant linear	k_1	$[\text{N/m}]$	49	409
- nonlinear	k_3	$[\mu\text{N}/(\mu\text{m})^3]$	3.9	31
Frequency, 1. mode	f	$[\text{kHz}]$	466	1537
Effective Mass (Eq. 3)	m	$[10^{-12} \text{ kg}]$	5.72	4.39
Capacitance	C_w	$[\text{fF}]$	7.14	7.14
Mechanical capacit.	C_m	$[\text{aF}]$	10.4	12.5
Mechanical inductance	L_m	$[\text{H}]$	1120	860
Mechanical resistance	R_m	$[\text{k}\Omega]$	164	415

Table 1: Simulation results for test resonators.

$$R_m = \frac{\sqrt{km}}{Q\eta^2},$$

$$L_m = \frac{m}{\eta^2} \text{ and}$$

$$C_m = \frac{\eta^2}{k},$$

where Q is mechanical quality factor of the resonator and η is electromechanical coupling factor

$$\eta = V_{DC} \frac{fC_w}{fx},$$

where C_w is the working capacitance between single electrode and the resonating beam. Using the FEM-calculated ($L_e=100 \mu\text{m}$) values for k and m , and assuming $Q=20000$ and DC-bias voltage $V_{DC}=10 \text{ V}$, component values of the equivalent electrical circuit are calculated (Equations 5-6) into Table 1. The capacitance value $C_w=7.14 \text{ fF}$ is also simulated by FEM

The equivalent circuit shown in Figure 6 is valid if the amplitude of vibration is small (vibration is in linear region). In nonlinear region harmonic balance (HB) method has been used to solve the non-linear components included in the model by third-order mechanical non-linearity [7].

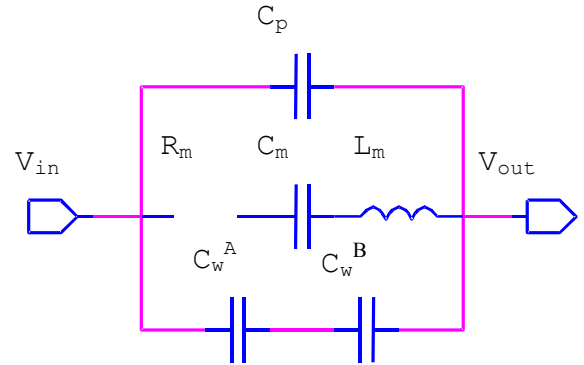


Figure 6: Equivalent circuit for the modeled resonator operating in linear regime.

3 EXPERIMENTAL

The dimensions of the two prototype bridge resonators used in measurements correspond to the values in Table 1. The resonator structures were manufactured using SOI-wafer (type-II resonator is shown Figure 7). Thickness of the SiO_2 was $1 \mu\text{m}$. The size of the air gaps was $d = 1 \mu\text{m}$ and electrical contacts were made by using $100 \mu\text{m} \times 100 \mu\text{m}$ contact pads. The parasitic substrate capacitance

induced by each pad was ~ 0.3 pF. Contributions to the parasitic capacitance C_p in the equivalent circuit model (Figure 2) are also due to the bond wires.

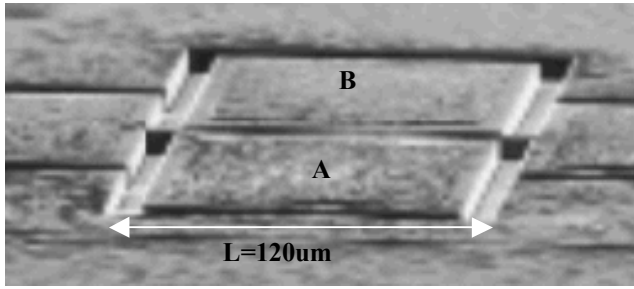


Figure 7: SEM-picture of type-II SOI-resonator.

The measurement was done using a network spectrum analyzer HP4195A. The beam was excited by electrode A using AC-voltage V_{in} and the output voltage was detected in electrode B. A symmetric DC-bias voltage between electrodes and resonator was $V_{DC} = 10$ V. Measured signal was preamplified to get higher signal to noise ratio.

Measured (markers) frequency response at two excitation V_{in} levels is shown in Figures 8 and 9 together with simulated results (solid lines). The lower excitation level $V_{in}=1$ mV corresponds to operation in linear regime, while in Figure 9 at $V_{in}=10$ mV the effect of third order mechanical non-linearity is visible. The good agreement between the simulated and measured response indicates that the simulation methods are able to accurately predict the resonator behavior. The quality factor extracted from the data is $Q \sim 30000$.

4 SUMMARY

Finite element method (FEM) has been used to calculate the mechanical parameters for a clamped-clamped beam micromechanical resonators. The calculated values are used in creating equivalent electrical circuit model for the resonator structures, including effects due to mechanical non-linearity. Good agreement is found between the measured and simulated resonator frequency responses. Q -value of the order of 30000 has been extracted for 1.5 MHz clamped-clamped SOI-resonator.

ACKNOWLEDGEMENTS

Discussions with T. Veijola, T. Ryhänen and H. Kuisma are acknowledged.

REFERENCES

- [1] HUT Circuit Theory Laboratory, Aug 18 1999, [referred: Jan 15 2000]
><http://www.aplac.hut.fi/aplac/>
- [2] J. Weigold, A.-C. Wong, C. Nguyen, S. Pang, Journal of Microelectromechanical Systems, 8 3, 221-228, 1999.

[3] R. Buser, Sensors and Actuators, A21-23, 323-327, 1990.

[4] O. Tabata, T. Yamamoto, A. Seshia and R. Howe, Transducers '99, Digest of Technical Papers, 2, 1538-1541, 1999.

[5] Y. Yoshii, A. Nakajo, H. Abe, K. Ninomiya, H. Miyashita, N. Sakurai, M. Kosuge and S. Hao, Transducers '97, Digest of Technical Papers, 2, 1485-1488, 1997.

[6] K. Kihong, K. Kenneth, Interconnect Technology Conference, Proceedings of the IEEE 1998 International, 21-23, 1998.

[7] T. Veijola, T. Mattila, O. Jaakkola, J. Kiihamäki, T. Lamminmäki, A. Oja, K. Ruokonen, H. Seppä, P. Seppälä and I. Tittonen, Technical paper, International Microwave Symposium, IEEE Microwave Theory and Techniques Society, 1999.

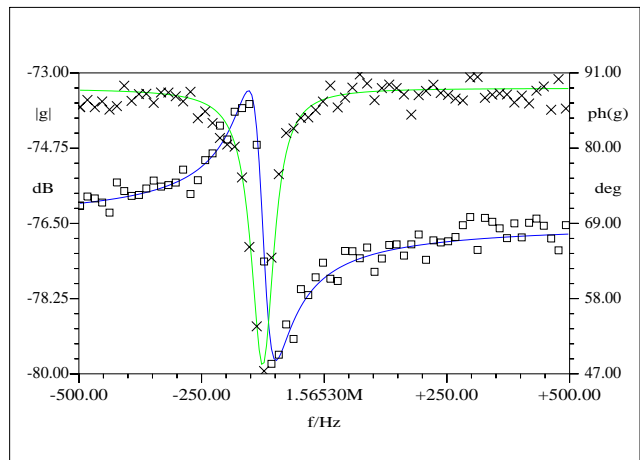


Figure 8: Simulated (lines) and measured (markers) data for the type-II resonator at $V_{in}=1$ mV.

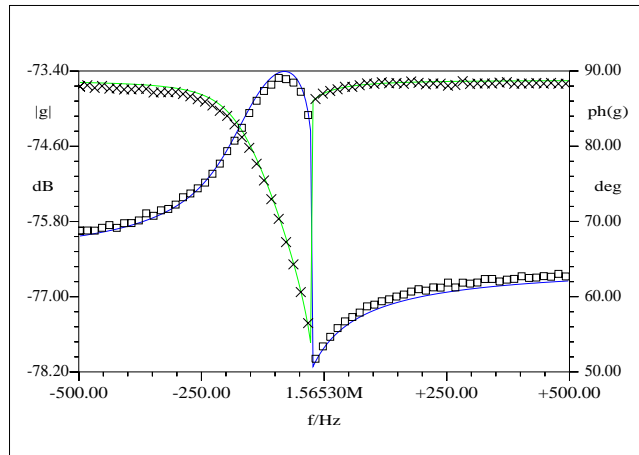


Figure 9: Comparison between the simulated (lines) and measured (markers) data for type-II resonator ($V_{in}=10$ mV).